

# Structure and Racemization of Optically Active *mer*-(3-Azapentane-1,5-diamine or 3-methyl-3-azapentane-1,5-diamine)(ethylenediamine-*N*-acetato)cobalt(III) Complexes

Hiroshi KAWAGUCHI,\* Hironobu FUKAKI, Tomoharu AMA, Takaji YASUI,  
Ken-ichi OKAMOTO,\*† and Jinsai HIDAKA†

Department of Chemistry, Faculty of Science, Kochi University, Akebono-cho, Kochi 780

†Department of Chemistry, University of Tsukuba, Tsukuba, Ibaraki 305

(Received February 3, 1988)

The crystal structure of  $(-)^{CD}_{500}mer-[Co(edma)(dien)]Br_2 \cdot 2/3CH_3OH \cdot 2/3H_2O$  was determined by the X-ray diffraction method. The crystal is triclinic, space group  $P1$ ,  $a=13.824(8)$ ,  $b=13.814(8)$ ,  $c=8.055(3)$  Å,  $\alpha=101.18(6)$ ,  $\beta=101.17(6)$ ,  $\gamma=116.32(5)^\circ$ , and  $Z=3$ . All of the crystallographically independent complex cations, in which the terdentate ligands coordinate meridionally, have a  $\delta$  spiral configuration, and the asymmetric nitrogen donor atoms of the edma ligands take an *S* configuration. The racemization reactions due to the inversion at the secondary amine nitrogen atom of the edma ligand in  $(-)^{CD}_{500}mer-[Co(edma)(dien)]^{2+}$  and  $(-)^{CD}_{514}mer-[Co(edma)(mdien)]^{2+}$  were studied at 20–35 °C in the pH range of 6.10–7.24. The rate law for both complexes was described as  $R=k[OH^-][\text{complex}]$ . The activation parameters at 30.0 °C were  $\Delta H^\ddagger$  of 94.9 kJ mol<sup>-1</sup> and  $\Delta S^\ddagger$  of 126 J K<sup>-1</sup> mol<sup>-1</sup> for the dien complex and  $\Delta H^\ddagger$  of 73.8 kJ mol<sup>-1</sup> and  $\Delta S^\ddagger$  of 62.0 J K<sup>-1</sup> mol<sup>-1</sup> for the mdien complex.

Four possible geometrical isomers for each of  $[Co(edma)(dien)]^{2+}$  and  $[Co(edma)(mdien)]^{2+}$  (edma, dien, and mdien denote ethylenediamine-*N*-acetate, 3-azapentane-1,5-diamine, and 3-methyl-3-azapentane-1,5-diamine, respectively) have been separated and resolved into their optically active isomers.<sup>1)</sup> Two pairs of enantiomers are possible for *mer*- $[Co(edma)(dien)]^{2+}$  and *mer*- $[Co(edma)(mdien)]^{2+}$  as shown in Fig. 1, where the enantiomers are designated by the combination of the *R* or *S* configuration due to the asymmetric nitrogen atom of the edma ligand and the  $\delta$  or  $\lambda$  spiral configuration due to the arrangement of the two trans N–H groups in *mer*- $[Co(edma)(dien)]^{2+}$  or due to the arrangement of the trans N–H and N–CH<sub>3</sub> groups in *mer*- $[Co(edma)(mdien)]^{2+}$ . However, it is difficult to determine spectrochemically their absolute configurations, and then we determined

the crystal structure of  $(-)^{CD}_{500}mer-[Co(edma)(dien)]Br_2 \cdot 2/3CH_3OH \cdot 2/3H_2O$  by the X-ray diffraction method. A preliminary report has been presented.<sup>2)</sup>

Similar cases have been reported for *mer*- $[Co(aepn)(dien)]^{3+}$  (aepn; 3-azahexane-1,6-diamine) and *mer*- $[Co(dien)_2]^{3+}$ . Two pairs of enantiomers are possible for *mer*- $[Co(aepn)(dien)]^{3+}$  and the absolute configuration of the  $(-)^{CD}_{474}$  isomer has been determined by Ishii et al.<sup>3)</sup> On the other hand, a pair of enantiomers are possible for *mer*- $[Co(dien)_2]^{3+}$  and designated as  $\delta$  and  $\lambda$  spiral configurations. Their absolute configurations have been determined by Okiyama et al.<sup>4)</sup> The kinetics of racemization due to  $\delta$  spiral  $\rightleftharpoons$   $\lambda$  spiral change for *mer*- $[Co(dien)_2]^{3+}$  has been studied by Searle and Keene.<sup>5)</sup> The bis(dien) complex racemizes with inversion<sup>6)</sup> at one of the two secondary amine nitrogen (sec-N) centers. The racemization process was described by a rate law of  $R=k[OH^-][\text{complex}]$ , and a mechanism of Scheme 1 has been proposed.

In the case of *mer*- $[Co(edma)(dien)]^{2+}$ , the inversion at the sec-N center in the coordinating edma results in *S*( $\delta$  spiral)  $\rightleftharpoons$  *R*( $\lambda$  spiral) or *S*( $\lambda$  spiral)  $\rightleftharpoons$  *R*( $\delta$  spiral) change (racemization) (Fig. 1). While, the inversion at the sec-N center in the coordinating dien results in *S*( $\delta$  spiral)  $\rightleftharpoons$  *S*( $\lambda$  spiral) or *R*( $\delta$  spiral)  $\rightleftharpoons$  *R*( $\lambda$  spiral) change (epimerization); the vicinal CD contribution due to the asymmetric sec-N of the coordinating edma

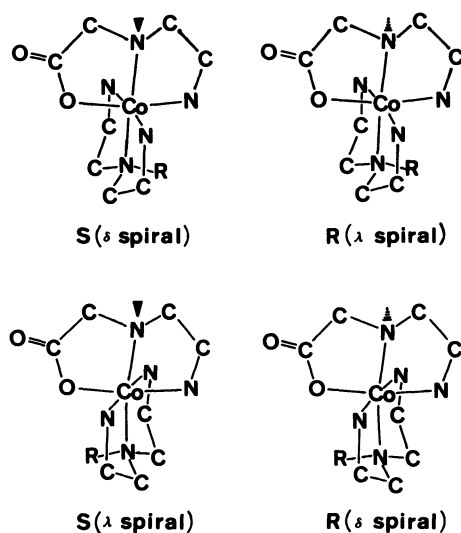
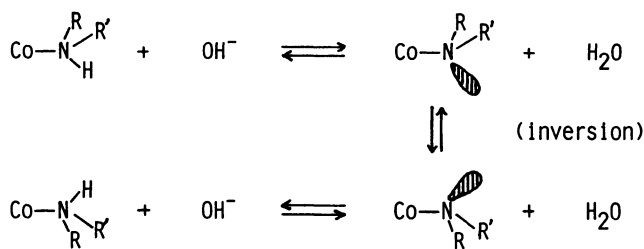


Fig. 1. Two pairs of enantiomeric isomers in *mer*- $[Co(edma)(dien)]^{2+}$  ( $R=H$ ) and *mer*- $[Co(edma)(mdien)]^{2+}$  ( $R=CH_3$ ).



Scheme 1.

remains. These configurational changes must involve the dissociation of the N–H bonds.<sup>5)</sup> Therefore, in the case of *mer*-[Co(edma)(mdien)]<sup>2+</sup> only inversion at the sec-N center in the coordinating edma is possible; racemization occurs. The present paper is concerned with the structure and racemization of the two *mer* edma complexes.

### Experimental

**Complexes.** The complexes used in the present work were prepared and resolved according to the methods described in our previous paper:<sup>1)</sup> (–)<sub>500</sub><sup>CD</sup>-*mer*-[Co(edma)(dien)]Br·2/3CH<sub>3</sub>OH·2/3H<sub>2</sub>O ( $\Delta\epsilon_{500}=-0.437$ ,  $\Delta\epsilon_{450}=+0.705$ ), (–)<sub>514</sub><sup>CD</sup>-*mer*-[Co(edma)(mdien)]Cl<sub>2</sub>·H<sub>2</sub>O ( $\Delta\epsilon_{514}=-0.490$ ,  $\Delta\epsilon_{460}=+0.730$ ).

**Racemization.** The racemization reactions were followed spectropolarimetrically with a JASCO J-22 spectropolarimeter. A reaction vessel with a jacket and a water-jacket cell mounted in the cell compartment of the spectropolarimeter were thermostated at a constant temperature ( $\pm 0.1$  °C) with circulating water from a constant-temperature bath. During the kinetic runs, the temperature and the pH of the reaction solution were checked with a thermistor-type thermometer (Takara D-221) and a pH meter (Toa TSC-10A), respectively. The reaction was started by dissolving the complex in 20 cm<sup>3</sup> of a buffered solution in the reaction vessel. About 3 cm<sup>3</sup> of this solution was quickly transferred into the cell in order to record the decrease of the CD intensity at a suitable

wavelength (450 nm for *mer*-[Co(edma)(dien)]<sup>2+</sup> and 460 nm for *mer*-[Co(edma)(mdien)]<sup>2+</sup>). The following conditions were set: pH 6.0–7.0 (Na<sub>2</sub>HPO<sub>4</sub>–KH<sub>2</sub>PO<sub>4</sub> and collidine–HNO<sub>3</sub> buffers), complex concentration  $1.8 \times 10^{-3}$  M (M=mol dm<sup>-3</sup>), ionic strength 1.0 M (NaNO<sub>3</sub>), and temperature 19.9–40.0 °C. The ionic product of water at the appropriate temperature was obtained from the literature<sup>7)</sup> and the appropriate activity coefficient corrections for ionic strength were made using the data from the same source. The hydroxide concentration could then be calculated.

For the racemization processes of both *mer*-[Co(edma)(dien)]<sup>2+</sup> and *mer*-[Co(edma)(mdien)]<sup>2+</sup>, plots of  $\ln[(L_0 - L_{eq})/(L_t - L_{eq})]$  vs. time, where  $L$  represents the CD intensity at the subscripted time, gave straight lines over three half-lives, from which the pseudo-first-order rate constant  $k_{obsd}(s^{-1})$  were obtained. Analyses of the kinetic data were carried out on an NEC PC-9801F computer using the least-squares method. In each of the kinetic data analysis, the value of the standard error was within  $\pm 1\%$  of the rate constant.

**X-Ray Data Collection.** Unit cell parameters and intensity data for the single crystal (ca. 0.30×0.32×0.63 mm<sup>3</sup>) were measured on a Rigaku-denki four-circle diffractometer (AFC-5) with graphite-monochromatized Mo K $\alpha$  radiation. The unit cell parameters were determined by a least-squares refinement based on 49 reflections ( $2\theta < 11.7^\circ$  and 25 ones;  $20^\circ < 2\theta < 25^\circ$ ). Systematic absences led to the space group *P1*. Crystal data: C<sub>8</sub>H<sub>22</sub>N<sub>5</sub>O<sub>2</sub>Br<sub>2</sub>Co·2/3CH<sub>3</sub>O·2/3H<sub>2</sub>O, M.W.=472.4, triclinic, space group *P1*,  $a=13.824(8)$ ,  $b=13.814(8)$ ,  $c=8.055(3)$  Å,

Table 1. Positional and Thermal Parameters (with e.s.d.'s)

Atom	x	y	z	$B_{eq}/\text{\AA}^2$ <sup>a)</sup>	Atom	x	y	z	$B_{eq}/\text{\AA}^2$ <sup>a)</sup>
CoA	0.4288	0.6477	0.2867	1.69	CB7	0.297(1)	1.028(1)	0.922(2)	3.11
OA1	0.2964(8)	0.5588(8)	0.347(1)	2.53	CB8	0.264(1)	1.107(1)	1.024(2)	3.42
OA2	0.2019(8)	0.5710(8)	0.538(1)	3.26	CoD	0.8508(2)	0.2956(2)	0.3100(3)	1.67
NA1	0.4784(9)	0.7490(9)	0.525(1)	2.12	OD1	0.8929(8)	0.4277(8)	0.501(1)	2.40
NA2	0.5736(9)	0.7566(10)	0.262(1)	2.23	OD2	1.0003(9)	0.5232(8)	0.787(1)	3.40
NA3	0.3479(9)	0.7165(10)	0.168(1)	2.28	ND1	0.9038(9)	0.2464(9)	0.498(1)	2.01
NA4	0.3759(10)	0.5349(10)	0.053(2)	2.59	ND2	0.8165(9)	0.1515(9)	0.144(1)	2.21
NA5	0.4962(10)	0.5558(9)	0.370(1)	2.40	ND3	0.9992(10)	0.3758(9)	0.269(1)	2.16
CA1	0.282(1)	0.611(1)	0.480(2)	2.25	ND4	0.7899(10)	0.3490(9)	0.130(1)	2.71
CA2	0.374(1)	0.740(1)	0.570(2)	2.43	ND5	0.6917(9)	0.2295(10)	0.324(2)	2.75
CA3	0.563(1)	0.871(1)	0.533(2)	2.97	CD1	0.960(1)	0.442(1)	0.650(2)	2.30
CA4	0.643(1)	0.849(1)	0.438(2)	2.96	CD2	0.997(1)	0.350(1)	0.647(2)	2.13
CA5	0.293(1)	0.649(1)	–0.033(2)	3.16	CD3	0.941(1)	0.163(1)	0.425(2)	2.68
CA6	0.266(1)	0.527(1)	–0.053(2)	2.92	CD4	0.840(1)	0.082(1)	0.250(2)	3.06
CA7	0.364(1)	0.428(1)	0.079(2)	3.22	CD5	0.987(1)	0.429(1)	0.123(2)	3.39
CA8	0.475(1)	0.462(1)	0.216(2)	3.31	CD6	0.893(1)	0.459(1)	0.134(2)	3.29
CoB	0.0767(2)	0.8735(2)	0.9113(3)	1.68	CD7	0.698(1)	0.363(1)	0.169(2)	2.91
OB1	0.1649(8)	0.8294(8)	1.059(1)	2.40	CD8	0.618(1)	0.250(1)	0.192(2)	3.68
OB2	0.1530(9)	0.7237(9)	1.238(1)	3.32	BR1	0.5328(2)	0.9458(2)	0.0710(3)	3.77
NB1	–0.0263(9)	0.8197(9)	1.047(1)	2.09	BR2	0.0446(2)	0.1914(2)	–0.0100(3)	3.72
NB2	–0.0333(9)	0.9073(9)	0.778(1)	2.06	BR3	0.5503(2)	0.6389(2)	0.8219(3)	3.55
NB3	0.0075(9)	0.7236(10)	0.722(1)	2.02	BR4	0.7204(2)	0.1741(2)	0.7238(3)	3.58
NB4	0.1894(10)	0.9335(10)	0.790(2)	2.66	BR5	0.7786(2)	0.6797(2)	0.3972(3)	3.74
NB5	0.1685(9)	1.0331(9)	1.087(1)	2.51	BR6	1.0855(2)	0.0039(2)	0.4553(3)	3.56
CB1	0.111(1)	0.763(1)	1.140(2)	2.28	CE1	0.279(5)	0.288(5)	0.639(8)	20.42 <sup>b)</sup>
CB2	–0.016(1)	0.727(1)	1.101(2)	2.34	CE2	0.419(4)	0.059(4)	0.576(7)	17.03 <sup>b)</sup>
CB3	–0.146(1)	0.784(1)	0.935(2)	2.77	OE1	0.298(3)	0.320(3)	0.490(5)	21.07 <sup>b)</sup>
CB4	–0.125(1)	0.885(1)	0.864(2)	3.11	OE2	0.407(4)	0.090(4)	0.432(6)	26.74 <sup>b)</sup>
CB5	0.072(1)	0.736(1)	0.588(2)	3.17	OW1	0.661(3)	0.436(3)	0.686(4)	18.45 <sup>b)</sup>
CB6	0.197(1)	0.831(1)	0.693(2)	2.74	OW2	0.452(4)	0.271(4)	0.808(5)	24.95 <sup>b)</sup>

a)  $B_{eq}=8\pi^2(U_{11}+U_{22}+U_{33})/3$ . b) Isotropic temperature factor.

$\alpha=101.18(6)$ ,  $\beta=101.17(6)$ ,  $\gamma=116.32(5)^\circ$ ,  $V=1282(2) \text{ \AA}^3$ ,  $D_x=1.835 \text{ g cm}^{-3}$ ,  $D_m=1.82 \text{ g cm}^{-3}$ ,  $Z=3$ , and  $\mu(\text{Mo } K\alpha)=60.08 \text{ cm}^{-1}$ .

The intensity data were collected by the  $\omega$ - $2\theta$  scan technique up to  $2\theta=60^\circ$  with scan rate of  $3^\circ \text{ min}^{-1}$ . The intensity data were converted to the  $F_o$  data in the usual manner. Absorption corrections were not applied. A total of 5001 independent reflections with  $|F_o|>3\sigma(|F_o|)$  of the measured 8064 reflections were considered as "observed" and used for the structure analysis.

**Determination of the Crystal Structure.** The X-ray analysis calculations were carried out on a FACOM M-382 computer at University of Tsukuba. The positions of three cobalt and six bromide atoms were determined by the direct method (program MULTAN<sup>9</sup> was used). The difference-Fourier maps based on the three cobalt and six bromide positions revealed the other all non-hydrogen atoms. The structure was refined by a full-matrix least-squares refinement using the positional parameters, the anisotropic thermal parameters of the non-hydrogen atoms of the complex ions, and the isotropic thermal parameters of the non-hydrogen atoms of the water molecules (program RFIN by Finger<sup>10</sup> was used). The atomic scattering factors for all the non-hydrogen atoms were taken from the literature.<sup>10</sup> The final residual values were  $R=0.049$  and  $R_w=0.058$ , respectively. We attempted to determine the absolute configuration of the complex ions by an anomalous-scattering technique. When the refinements were carried out by use of a set of the atomic parameters

containing the  $\delta$  spiral configuration of the complex cations, the residual values converged to  $R=0.047$  and  $R_w=0.056$ , respectively. On the contrary, the refinements in the enantiomeric atomic parameters (the  $\lambda$  spiral configuration) resulted in the residual values of  $R=0.054$  and  $R_w=0.062$ , respectively. These facts suggest that the former is probably the correct choice, namely, the complex cation takes the  $\delta$  spiral configuration. A similar relationship was observed for the determination of the absolute configuration for the cobalt(III) complexes.<sup>11,12</sup>

The final positional parameters are listed in Table 1. A list of structure factors (Table A) and anisotropic thermal parameters of non-hydrogen atoms (Table B) are kept at the Chemical Society of Japan as Document No. 8810.

## Results and Discussion

**Description of the Structure.** A perspective drawing of the [Co(edma)(dien)]<sup>2+</sup> cation (CoA species) is shown in Fig. 2, together with the numbering scheme. The bond distances and angles (with standard deviations) are summarized in Table 2. There are three crystallographically independent complex cations in an asymmetric unit, though their shapes and sizes remarkably resemble one another. The cobalt atom is octahedrally surrounded by an oxygen atom and five nitrogen atoms. The ethylenediamine-*N*-acetate and 3-azapentane-1,5-diamine coordinate meridionally to

Table 2. Interatomic Distances and Bond Angles (with e.s.d.'s) for  $(-)\text{Co}^{\text{III}}\text{-mer-[Co(edma)(dien)]Br}_2 \cdot 2/3\text{CH}_3\text{OH} \cdot 2/3\text{H}_2\text{O}$

(a) Bond distance ( <i>l</i> /Å)				O1–Co–N4	93.5(4)	93.5(6)	92.7(5)
				O1–Co–N5	88.7(5)	88.9(5)	88.2(5)
				N1–Co–N2	87.4(5)	86.7(6)	86.6(5)
A	B	D		N1–Co–N3	96.3(5)	95.6(5)	96.3(5)
Co–O1	1.92(1)	1.91(1)	1.91(1)	N1–Co–N4	175.4(6)	176.1(4)	175.3(6)
Co–N1	1.92(1)	1.93(1)	1.93(1)	N1–Co–N5	92.7(5)	93.4(5)	94.0(6)
Co–N2	1.98(1)	1.97(1)	1.96(1)	N2–Co–N3	91.0(5)	90.3(5)	90.4(5)
Co–N3	1.99(1)	1.99(1)	1.98(1)	N2–Co–N4	95.5(5)	96.1(6)	96.5(5)
Co–N4	1.96(1)	1.96(1)	1.96(1)	N2–Co–N5	92.1(6)	92.7(5)	92.6(5)
Co–N5	2.02(2)	2.02(1)	2.01(1)	N3–Co–N4	87.2(6)	87.1(5)	87.1(6)
O1–C1	1.27(2)	1.28(2)	1.29(2)	N3–Co–N5	170.6(4)	170.7(5)	169.4(6)
O2–C1	1.23(2)	1.23(2)	1.24(2)	N4–Co–N5	83.6(5)	83.8(5)	82.5(6)
N1–C2	1.51(2)	1.49(2)	1.50(1)	Co–O1–C1	115.9(8)	115.1(10)	115.0(11)
N1–C3	1.54(2)	1.52(2)	1.52(2)	Co–N1–C2	108.2(7)	108.3(11)	108.1(9)
N2–C4	1.50(2)	1.50(2)	1.49(2)	Co–N1–C3	108.9(9)	108.8(9)	109.6(9)
N3–C5	1.54(2)	1.52(2)	1.52(2)	C2–N1–C3	113.2(13)	114.0(10)	113.5(12)
N4–C6	1.54(2)	1.54(2)	1.55(2)	Co–N2–C4	107.9(9)	108.2(10)	108.8(8)
N4–C7	1.47(2)	1.47(1)	1.46(2)	Co–N3–C5	109.3(11)	109.5(8)	109.7(10)
N5–C8	1.49(2)	1.52(2)	1.48(2)	Co–N4–C6	105.9(10)	105.5(9)	105.4(9)
C1–C2	1.57(2)	1.55(2)	1.55(3)	Co–N4–C7	109.0(9)	109.1(10)	109.5(11)
C3–C4	1.56(3)	1.54(3)	1.56(2)	C6–N4–C7	115.3(10)	115.1(14)	114.8(13)
C5–C6	1.53(3)	1.55(2)	1.54(3)	Co–N5–C8	110.2(10)	109.9(9)	111.5(10)
C7–C8	1.52(2)	1.53(3)	1.54(2)	O1–C1–O2	126.5(11)	124.4(15)	125.3(17)
CE1–OE1	1.39(8)			O1–C1–C2	115.2(13)	115.7(15)	115.4(12)
CE2–OE2	1.32(8)			O2–C1–C2	118.3(14)	119.8(14)	119.2(14)
(b) Bond angle ( <i>φ</i> /°)				N1–C2–C1	104.2(13)	104.8(11)	105.0(12)
				N1–C3–C4	101.6(12)	102.4(10)	101.4(14)
A	B	D		N2–C4–C3	109.8(11)	108.8(16)	109.5(11)
O1–Co–N1	83.6(4)	83.8(5)	84.1(5)	N3–C5–C6	107.2(13)	106.4(11)	106.7(15)
O1–Co–N2	171.0(4)	170.4(5)	170.7(5)	N4–C6–C5	106.1(10)	105.8(15)	105.6(14)
O1–Co–N3	89.7(5)	89.6(5)	90.5(5)	N4–C7–C8	105.4(10)	105.5(13)	104.6(15)
				N5–C8–C7	106.8(15)	105.9(12)	105.7(11)

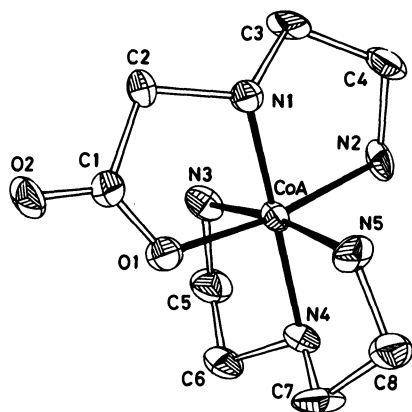


Fig. 2. Perspective view of  $(-)\text{Co}^{\text{III}}\text{-mer-[Co(edma)(dien)]}^{2+}$  ion.

the cobalt atom as terdentate ligands. For the  $\text{mer-[Co(edma)(dien)]}^{2+}$  isomers, two pairs of enantiomers are possible, where the enantiomers are designated by the combination of the *R* or *S* configuration due to the asymmetric nitrogen donor atom of the edma ligand and the  $\delta$  or  $\lambda$  spiral configuration due to the arrangement of the two trans N-H groups as in the case of  $\text{mer-[Co(ida)(dien)]}^+$  (ida; iminodiacetate).<sup>11</sup> The absolute configuration of the asymmetric nitrogen donor atom in the present complex cation, which has the  $\delta$  spiral configuration, was determined to be *S* (Fig. 2). This seems to indicate that one of two pairs of enantiomers, *S*( $\delta$  spiral) and *R*( $\lambda$  spiral) isomers, were selectively formed in the crystalline state, because both of the *R*( $\delta$  spiral) and *S*( $\lambda$  spiral) isomers have a significantly intramolecular steric interaction between the amino group in the edma ligand and the two methylene groups in the dien ligand.

The bond distances and angles for the coordinating dien in the three crystallographically independent complex cations are quite similar to those for  $\text{mer-[Co(mida)(dien)]}^{+11}$  and  $\text{mer-[Co(dien)}_2\text{)]}^{3+,4}$ . The bond distances and angles for the N1-O1 chelate moiety in the edma ligand also resemble to those for the cobalt(III) complexes with amino carboxylates,<sup>11-13</sup> although the Co-O1 distance (av. 1.91(1) Å) is somewhat longer and the Co-N1 one is somewhat shorter (av. 1.93(1) Å) than those of the corresponding distances. The conformations of the edma and dien ligands in the three complex cations resemble one another. The N1-O1 chelate ring in the edma ligand takes an envelope form with  $\lambda$  conformation as in the case of the cobalt(III) complexes with amino carboxylates,<sup>11-13</sup> and the diamine chelate ring N1-N2 takes an asymmetric skew form with  $\delta$  conformation. Two coupled chelate rings in the dien ligand take asymmetric skew forms with  $\delta$  and  $\lambda$  conformations, respectively, which somewhat differ from  $\text{mer-[Co(mida)(dien)]}^{+11}$  and  $\text{mer-[Co(dien)}_2\text{)]}^{3+,4}$ .

**CD Spectra.** Figure 3 shows the absorption and

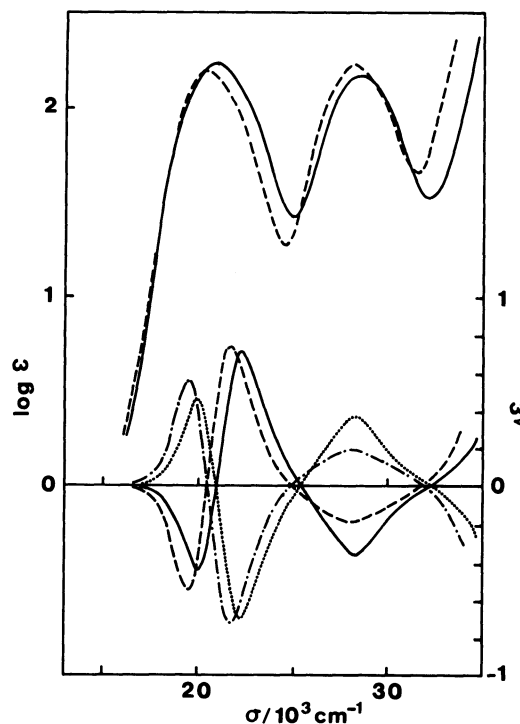


Fig. 3. Absorption (AB) and CD spectra:  $(-)\text{Co}^{\text{III}}_{500}$  (—) and  $(+)\text{Co}^{\text{III}}_{500}$  (.....) isomers of  $\text{mer-[Co(edma)(dien)]}^{2+}$  and  $(-)\text{Co}^{\text{III}}_{514}$  (---) and  $(+)\text{Co}^{\text{III}}_{514}$  (-.-.-) isomers of  $\text{mer-[Co(edma)(mdien)]}^{2+}$ . Solvent: water for AB measurements and 0.1 M HCl for CD measurements.

CD spectra of optically active  $\text{mer-[Co(edma)(dien)]}^{2+}$  and  $\text{mer-[Co(edma)(mdien)]}^{2+}$  measured in 0.1 M HCl at room temperature. These optically active isomers were stable in acidic solution and exhibited no measurable absorption and CD spectral changes. However, these isomers easily racemized in neutral or basic solution. Similar behavior was observed for the optically active isomers of complexes such as  $[\text{Co(sar)(NH}_3)_4]^{2+}$  (sar; sarcosinate anion)<sup>14</sup> and  $\text{mer-[Co(dien)}_2\text{)]}^{3+,5}$ . The CD curves of  $(+)\text{Co}^{\text{III}}_{500}$  and  $(-)\text{Co}^{\text{III}}_{500}$  isomers of  $\text{mer-[Co(edma)(dien)]}^{2+}$  are exactly symmetrical each other, indicating that these isomers are in an enantiomeric relation; the configuration of the  $(+)\text{Co}^{\text{III}}_{500}$  isomer is assigned to *R*( $\lambda$  spiral).

$(-)\text{Co}^{\text{III}}_{514}$  and  $(+)\text{Co}^{\text{III}}_{514}$ - $[\text{Co(edma)(mdien)]}^{2+}$  show very similar CD spectra to those for  $(-)\text{Co}^{\text{III}}_{500}$  and  $(+)\text{Co}^{\text{III}}_{500}$  dien analogues, respectively (Fig. 3). Accordingly, *S*( $\delta$  spiral) is assigned to the  $(-)\text{Co}^{\text{III}}_{514}$  isomer of  $\text{mer-[Co(edma)(mdien)]}^{2+}$  and *R*( $\lambda$  spiral) to the  $(+)\text{Co}^{\text{III}}_{514}$  one.

Both  $\text{mer-[Co(edma)(dien)]}^{2+}$  and  $\text{mer-[Co(edma)(mdien)]}^{2+}$  have two CD contributions, one from the spiral configuration and the other from the so-called vicinal effect due to the asymmetric sec-N in the edma ligand. The CD intensities in the first band region for these complexes are stronger than those for  $\text{mer-[Co(dien)}_2\text{)]}^{3+,5}$  and  $\text{mer-[Co(ida)(dien)]}^{+11}$  having only the CD contribution from the spiral configuration.

**Racemization.** Figure 4 shows CD spectral change

with time of  $(-)\text{ED}_{500}\text{-mer-[Co(edma)(dien)]}^{2+}$  in phosphate buffered solution at 39.9 °C. The initial CD curve almost coincided with the CD curve measured in 0.1 M HCl. The isocircular dichroism points lay on the base line and the values of CD intensities at various wavelengths decreased in the same ratio. The CD spectrum almost disappeared after 2 h. The absorption spectrum changed little during the CD measurement, indicating that no isomerization and/or decomposition occurred. In the  $(-)\text{ED}_{500}\text{-S}(\delta \text{ spiral})$  isomer of *mer*-[Co(edma)(dien)]<sup>2+</sup>, the inversion at the sec-N in the dien ligand brings about the  $S(\delta \text{ spiral}) \rightleftharpoons S(\lambda \text{ spiral})$  change (epimerization). In this case, however, the vicinal CD contribution due to the asymmetric sec-N of the edma ligand is expected to remain. On the other hand, the inversion at the sec-N center of the edma ligand leads to the  $S(\delta \text{ spiral}) \rightleftharpoons R(\lambda \text{ spiral})$  change (racemization). The CD decrease in Fig. 4 conforms to the  $S(\delta \text{ spiral}) \rightleftharpoons R(\lambda \text{ spiral})$  change, that is, the inversion at the sec-N of edma. This result, therefore, means that (1) the  $S(\delta \text{ spiral}) \rightarrow S(\lambda \text{ spiral})$  change is very slow compared with the  $S(\delta \text{ spiral}) \rightarrow R(\lambda \text{ spiral})$  change or (2) the  $S(\delta \text{ spiral}) \rightleftharpoons S(\lambda \text{ spiral})$  equilibrium extremely lies to the  $S(\delta \text{ spiral})$  side if the rate of the  $S(\delta \text{ spiral}) \rightarrow S(\lambda \text{ spiral})$  change is comparable to that of the  $S(\delta \text{ spiral}) \rightarrow R(\lambda \text{ spiral})$  change. In  $(-)\text{ED}_{514}\text{-mer-[Co(edma)(mdien)]}^{2+}$ , only the inversion at the sec-N center of the edma ligand is expected to occur. In fact, this complex showed the decrease of the CD intensity in the same pattern as  $(-)\text{ED}_{500}\text{-[Co(edma)(dien)]}^{2+}$  did.

The progress of the racemization was followed by monitoring the decrease of the CD intensity at 450 nm

for *mer*-[Co(edma)(dien)]<sup>2+</sup> and at 460 nm for *mer*-[Co(edma)(mdien)]<sup>2+</sup>. Kinetic data are summarized in Table 3. The values of the racemization rate constant  $k(=k_{\text{obsd}}/[\text{OH}^-])$  for *mer*-[Co(edma)(dien)]<sup>2+</sup> at 39.9 °C are essentially constant, so the rate law is described as  $R=k[\text{OH}^-][\text{complex}]$ . Activation energies  $E_a$  were computed by least-squares analysis of the Arrhenius plots of  $k$ . The activation parameters calculated for the two complexes are given in Table 4. The close similarity in the activation parameters between the *mer*-[Co(edma)(dien)]<sup>2+</sup> and *mer*-[Co(dien)<sub>2</sub>]<sup>3+</sup> complexes, as compared in Table 4, strongly suggests that a common mechanism takes place (Scheme 1). The racemization rate of *mer*-[Co(edma)(dien)]<sup>2+</sup> is about twice faster than that of *mer*-[Co(dien)<sub>2</sub>]<sup>3+</sup>. The difference in the rates of racemization might be explained by the electronic and conformational properties of the chelates. The electronegative carboxyl group decreases the electron density on the sec-N center. Consequently, the pre-equilibrium of Scheme 1 displaces to the deprotonated form and the rate of racemization increases. The glycinate chelate ring in *mer*-[Co(edma)(dien)]<sup>2+</sup> has a little conformational deformation out of the N-Co-O plane, whereas the ethylenediamine chelate rings in *mer*-[Co(dien)<sub>2</sub>]<sup>3+</sup> is markedly puckered; therefore, the conformational interchange may be easier in the edma ring than in the dien ring for *mer*-[Co(edma)(dien)]<sup>2+</sup>.

The racemization rate of *mer*-[Co(edma)(mdien)]<sup>2+</sup> is about one order faster than that of *mer*-[Co(edma)(dien)]<sup>2+</sup> (Table 3), and the activation enthalpy of the former is smaller than that of the latter (Table 4). It seems likely that the electron donative

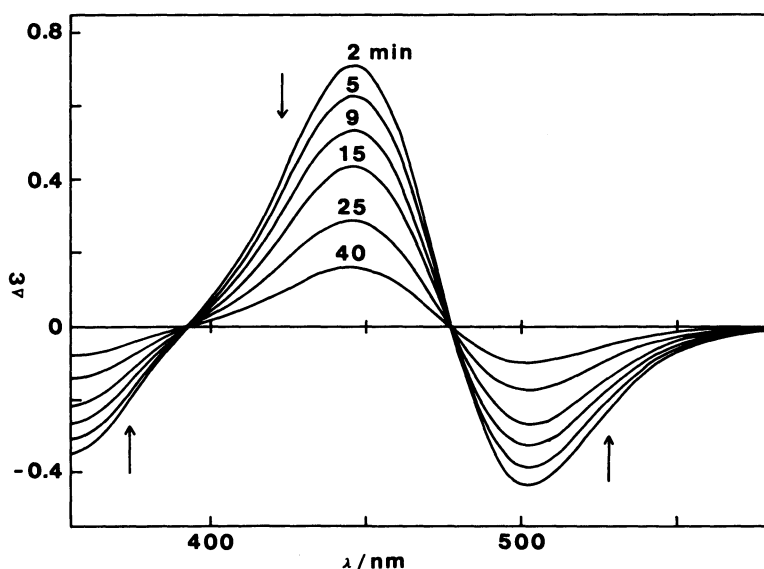


Fig. 4. The CD spectral change of  $(-)\text{ED}_{500}\text{-mer-[Co(edma)(dien)]}^{2+}$  measured under the conditions of pH 7.06 (phosphate buffer), ionic strength 1.0 M ( $\text{NaNO}_3$ ), and 39.9 °C. The curves show the spectra measured at 2, 5, 9, 15, 25, and 40 min.

Table 3. The Rate Constants for Racemization of *mer*-[Co(L<sub>1</sub>)(L<sub>2</sub>)]<sup>n+</sup> Ions in Phosphate Buffered Solutions

Complex	<i>T</i>	pH	<i>k</i> <sub>obsd</sub>	<i>k</i>
	°C		10 <sup>-4</sup> s <sup>-1</sup>	10 <sup>2</sup> M <sup>-1</sup> s <sup>-1</sup>
[Co(edma)(dien)] <sup>2+</sup> <sup>a)</sup>	30.0	7.05	0.464	2.16
	34.9	7.09	1.40	4.15
	39.9	7.05	3.18	7.36
	39.9	7.09	3.36	7.09
	39.9	6.45	0.803	7.40
	39.9	6.10	0.360	7.43
	39.9	7.24	2.69	4.48 <sup>c)</sup>
[Co(edma)(mdien)] <sup>2+</sup> <sup>a)</sup>	30.0	7.15	4.43	16.4
	25.0	7.12	1.66	9.61
	19.9	7.11	0.686	6.01
[Co(dien) <sub>2</sub> ] <sup>3+</sup> <sup>b)</sup>	35	6.42	0.086	1.54
	40	6.44	0.297	3.6
	40	7.31	2.89	4.7 <sup>c)</sup>

a) *I*=1.0 M(NaNO<sub>3</sub>). b) Reference 5. *I*=2.0 M(NaNO<sub>3</sub>). c) Collidine buffer.

Table 4. The Activation Parameters for Racemization of *mer*-[Co(L<sub>1</sub>)(L<sub>2</sub>)]<sup>n+</sup> Ions

Complex	<i>T</i>	$\Delta H^*$	$\Delta S^*$
	°C	kJ mol <sup>-1</sup>	J K <sup>-1</sup> mol <sup>-1</sup>
[Co(edma)(dien)] <sup>2+</sup> <sup>a)</sup>	34.9	94.8±3.3	125±10
[Co(edma)(mdien)] <sup>2+</sup> <sup>a)</sup>	30.0	73.8±4.0	62.0±13.5
[Co(dien) <sub>2</sub> ] <sup>3+</sup> <sup>b)</sup>	35	98.3±1.7	121±8.4

a) Phosphate buffer. *I*=1.0 M(NaNO<sub>3</sub>). b) Reference 5. Collidine-HNO<sub>3</sub> buffer. *I*=2.0 M(NaNO<sub>3</sub>).

CH<sub>3</sub> group exerts a trans effect in *mer*-[Co(edma)-(mdien)]<sup>2+</sup>, enhancing the racemization rate.

The racemization of optically active [Co(sar)-(NH<sub>3</sub>)]<sup>2+</sup> has been studied in a number of buffers.<sup>14)</sup> The rate was about twice slower in phosphate buffer rather than in collidine buffer, and this feature was rationalized on the basis of ion pairing; the complex reacts with the phosphate anion (HPO<sub>4</sub><sup>2-</sup> or H<sub>2</sub>PO<sub>4</sub><sup>-</sup>) to give an ion pair which no longer reacts with OH<sup>-</sup> at a rate comparable to that of the original complex, so that the racemization rate would be consequently diminished. In the case of [Co(dien)<sub>2</sub>]<sup>3+</sup>, the racemization rate in phosphate buffer was also slower than that in collidine buffer, but the difference between their rates was slight. However, in the present complex, the reverse tendency is observed (Table 3), so that the proposal given in the case of the racemization reaction of [Co(sar)(NH<sub>3</sub>)<sub>4</sub>]<sup>2+</sup> is inapplicable to the racemization reaction of the present complex. The reason is unknown at present. The studies for the factors such as the orientation of the complex ion in the ion pairing and the catalytic ability of phosphate anion may be required.

## References

- 1) T. Yasui, T. Shikiji, N. Koine, T. Ama, and H. Kawaguchi, *Bull. Chem. Soc. Jpn.*, **60**, 595 (1987).
- 2) K. Okamoto, T. Yasui, and J. Hidaka, *Chem. Lett.*, **1987**, 1561.
- 3) M. Ishii, S. Sato, Y. Saito, and M. Nakahara, *Bull. Chem. Soc. Jpn.*, **57**, 3094 (1984).
- 4) K. Okiyama, S. Sato, and Y. Saito, *Acta Crystallogr., Sect. B*, **35**, 2389 (1979).
- 5) G. H. Searle and F. R. Keene, *Inorg. Chem.*, **11**, 1006 (1972).
- 6) We use the term "inversion" here to describe the configurational change about a sec-N center in meridionally coordinated dien.
- 7) H. S. Harned and W. J. Hamer, *J. Am. Chem. Soc.*, **55**, 2194 (1933).
- 8) G. Germain, P. Main, and M. M. Woolfson, *Acta Crystallogr., Sect. A*, **27**, 368 (1971).
- 9) L. W. Finger, RFINE-2, Geophysical Lab. Carnegie Institute, Washington, D. C. (1972).
- 10) a) "International Tables for X-Ray Crystallography," Kynoch Press, Birmingham (1974). Vol. IV; b) D. T. Cromer and J. B. Mann, *Acta Crystallogr., Sect. A*, **24**, 321 (1968).
- 11) K. Okamoto, T. Yasui, and J. Hidaka, *Chem. Lett.*, **1987**, 551.
- 12) K. Okamoto, M. Suzuki, H. Einaga, and J. Hidaka, *Bull. Chem. Soc. Jpn.*, **56**, 3513 (1983).
- 13) K. Okamoto, K. Matsutani, and Y. Fujii, *Bull. Chem. Soc. Jpn.*, **58**, 3486 (1985).
- 14) B. Halpern, A. M. Sargeson, and K. R. Turnbull, *J. Am. Chem. Soc.*, **88**, 4630 (1966).